Analysis and Detection of Inter Turn Short Circuit Fault through Extended Self-Commissioning

Yuan Qi[1], Mohsen Zafarani[1], Bilal Akin[1], Steve Fedigan[2]

Electrical Engineering Department, University of Texas-Dallas[1]; Texas Instruments Inc.[2]

Abstract— **This paper presents a comprehensive analysis of PMSM stator winding impedance variation in inter turn short circuit and eccentricity faults. The phase impedances are monitored through an extended self-commissioning procedure at standstill mode before or after operation, and hence agnostic to well-known issues caused by transients, load/speed level or controller coefficient dependency. Moreover, the effect of stator iron core saturation on the electric parameters analyzed in depth. In order to distinguish the inter turn shorts from the eccentricity fault which exhibits similar behaviors, a classification algorithm based on the saturation effect is introduced and analyzed on the machines with different pole-slot combinations. Both 2-D FEA simulation and experimental test results are provided to show the efficacy of this analysis.**

Index Terms—**Eccentricity fault, electric parameter, inter turn short circuit fault, magnetic saturation, permanent magnet synchronous machines. (PMSMs)**

I. INTRODUCTION

THE trend in deployment of permanent magnet synchronous machines (PMSMs) has been remarkably increasing due to superior features such as high efficiency, high power density and high torque density. Thanks to these merits, today is permanent magnet machines have been used in various applications, including down-hole tractors, wind generation systems, electric vehicles (EVs) to name a few. As the use and diversity of applications increase, the fault diagnosis of PMSMs becomes an essential engineering field to improve reliability, optimize operational cost and estimate useful lifetime of drive systems. The most common PMSM fault types reported in industry are inter turn short circuit faults, permanent magnet (PM) demagnetization, rotor eccentricity and bearing failures. These faults may occur due to inherent manufacturing imperfections, harsh operating conditions, improper loading and component degradation. The impending faults not only affect the performance of machine is drive system but also reduce the overall system reliability, which may cause significant operation loss or even catastrophic faults. For instance, if a down hole tractor used in a typical oil production system fails, it takes one week to fix and restart the system where operation loss/day can be as high as $1M. Therefore, it is important to perform the fault diagnosis for optimized, reliable and safe operations.

This paper mainly focuses on practical diagnosis methods for the inter turn short circuit fault which is one of the most common fault observed in the field. The inter turn short circuit fault are mostly caused by stator winding insulation failure due to mechanical stress, overcurrent, moisture or thermal impact [1]. The short circuit faults cause unbalance in electric field and thus it may generate vibration and harmonics which can significantly reduce the system performance. The shorted turns create negative *d*-axis current component which leads to demagnetization of rotor magnets. Furthermore, the current circulated in the shorted coils may be very large and hence it can increase the electrical and thermal stress leading to a major insulation failure on the stator windings due to introduced hot spots. At the next stage, it may result in a phase to phase short circuit fault or phase to ground short circuit fault. Therefore, it is essential to propose reliable and practical methods to detect inter turn short circuit fault in PMSMs.

Recently, inter turn short circuit fault detection has been studied from various perspectives. The most popular one is motor current signature analysis (MCSA). It is well developed for *ac* induction machines and offers online monitoring without additional sensors for diagnosis [2]. It is also widely used in the fault diagnosis for PMSMs as well. In [3]-[7], the stator current is analyzed through fast Fourier transforms (FFT) and certain harmonics of stator current are considered as the fault indicator. Since, the inter turn short circuit fault increases the unbalance of the three phase winding, the even harmonics in rotor reference frame can also be used as fault indicator [8]-[12]. Similar to MCSA, the back-emf also analyzed in frequency domain with searching coils [13] and back-emf estimators in [14] and [15]. In [16], the detection based on the negative sequence voltage on stationary reference frame is proposed. In [17], the zero sequence component of different winding types are tested for inter turn short circuit analysis. According to the amplitude and phase angle variation in zero sequence component, the inter turn short circuit fault can be identified. In [18] and [19], the phase current amplitude is analyzed under faulty condition. Due to the shorted turns, the phase current is forced to increase in order to produce torque difference. In [20], the input impedance is used as the fault indicator and monitored by external circuit. However, there are some minor risks involved in these approaches especially when implemented through spectrum analysis where Fourier transformation is required for obtaining the feature of short circuit fault. First, it has low flexibility since the window function is fixed. Thus, MCSA needs sample current information at steady state, where the motor runs at constant speed with constant mechanic loads [21], whereas, in many practical adjustable speed motor drive applications,

stationary conditions cannot be assured for the online diagnosis. In order to overcome this drawback, the continuous wavelet transform (CWT) is used to analyze the phase current [22], phase voltage [23], q-axis voltage reference [24] for diagnosis in transient states. Other time-frequency methods are also implemented on the inter turn short circuit fault detection, including Hilbert-Huang transform (HHT) [25] [26], wavelet packet decomposition [27] [28] and short-time Fourier transform [29] [20]. In some of these proposed algorithms, the characteristics of the fault signatures are highly operating point dependent. In another word, with different load/speed, the amplitude of the signatures varies. Therefore, determining a dynamic threshold that is valid for all the operating points is a bit challenging task.

A diagnosis procedure covering all combinations is possible yet requires very high processing power to perform the analysis. Another critical shortcoming of spectral analysis is that the fault signatures are highly topology dependent and do not provide the same result for PM motors with different winding configurations [31]. However, the inter turn short circuit fault deeply affect the motor parameters. Therefore it is possible to detect the fault through motor parameter changes. In [32]-[34], high frequency signal injection and in [35] online saliency monitoring methods are given. These methods are firstly designed for the position estimation in sensorless control. The modeling techniques and finite elements analysis (FEA) of the inductance variance in fault condition are given in [36]. In [37] and [38], a complementary off line method is proposed for PM demagnetization fault and rotor eccentricity. It introduces the differential inductance for fault diagnosis of PMSMs requiring potentially low computation work load for controller. Different types of faults have different effects on the PMSMs electric parameters. Hence, it is critical to distinguish and classify the types of faults from different parameter signatures. In [39], the inter turn short circuit is analyzed from a similar perspective. It provides a tool to detect the inter turn short circuit fault of PMSMs with distributed stator windings. As an extension of these, this paper proposes an offline diagnosis method based on impedance analyses at start-up to detect inter turn short circuit fault in PMSMs with concentrated winding. Taking stator resistor into account significantly helps to identify and discern different fault types. This paper focuses on the stator winding impedance variation in inter turn short circuit fault PMSM based on parameter based self-commissioning at stationary conditions. The impedance analysis can perform at start-up and taking stator resistance into account significantly helps to identify and discern different fault type. Furthermore,
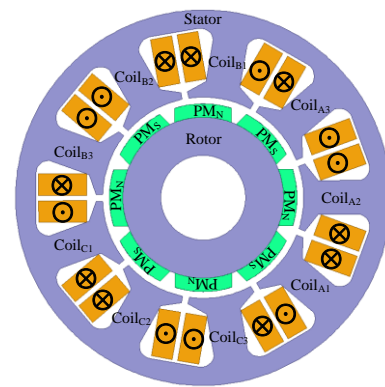

Fig. 1. Healthy PMSM structure used both in simulations and experiment

the eccentricity fault exhibiting similar faulty signatures and the effect of different pole/slot combinations are also analyzed in this paper. The feasibility of using stator winding impedance to identify the inter turn short circuit fault is validated through 2-D FEA simulation and experimental results. The advantages of this method is listed below,

- Easy to implement due to low computational complexity and CPU bandwidth requirements
- As a start-up procedure, it is not affected by system dynamics such as transients, load/speed level etc…
- It is independent from different pole/slot combinations
- Does not depend on the controller parameters which can significantly suppress and modify the fault signatures in current based diagnosis
- Takes the non-linearity and saturation phenomenon into account rather than relying on a linear model.

The structure of this paper is as follows: Section II focuses on the theoretical analysis of electric parameter in inter turn short circuit fault of PMSMs and introduces the method of estimation. Section III describes the iron core saturation effect on the electric parameters and gives the principle for distinguishing inter turn short circuit faults from other types of faults in different stator winding structures. Section IV provides the experiment setup and corresponding results.

II. ANALYSIS OF PMSMs WITH INTER TURN SHORT CIRCUIT FAULT

A. Analysis of Stator Winding Impedance

Fig.1 shows the 2-D model of the test PMSM, a three phase surface-mount PMSM with 8 poles used in simulation and experiments. Each phase has 3 coils in series and they are arranged in 9 slots in double layer configuration. The three phase windings are star connected. The electrical equation of a healthy coil can be written as following:

$$v_{a1H} = r_{a1H}i_{a1H} + L_{a1H}\frac{di_{a1H}}{dt} \qquad (1)$$

where

v_{a1H} : excitation voltage in healthy case.
i_{a1H} : current in healthy coil$_{A1}$.
r_{a1H} : resistance of healthy coil$_{A1}$.
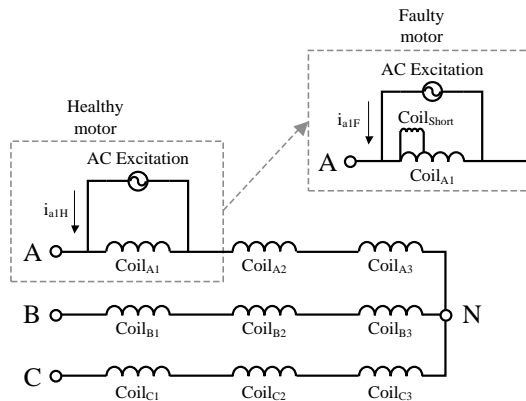L_{a1H} : self-inductance of healthy coil$_{A1}$.

Fig.2. Equivalent circuit of healthy PMSM and inter turn short circuit fault PMSM
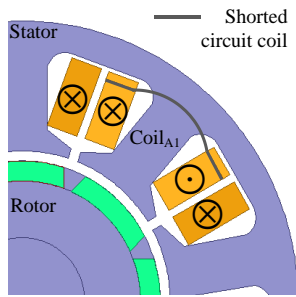

Fig.3. PMSM structure with inter turn short circuit fault

Correspondingly, if there is inter turn short circuit fault on coil$_{A1}$, as shown in Fig.2 and Fig.3, the equivalent circuit with hypothetical *ac* excitation are given by (2) and (3).

$$v_{a1F} = r_{a1F}i_{a1F} + L_{a1F}\frac{di_{a1F}}{dt} + L_{sa1F}\frac{di_s}{dt} \quad (2)$$

$$0 = r_s i_s + L_s \frac{di_s}{dt} + L_{a1s}\frac{di_{a1F}}{dt} \quad (3)$$

where

v_{a1F} : excitation voltage in faulty case.
i_{a1F} : current in faulty coil$_{A1}$.
i_s : current in short circuit winding.
r_{a1F} : resistance of faulty coil$_{A1}$.
r_s : resistance of short circuit coil.
L_{a1F} : self-inductance of faulty coil$_{A1}$.
L_s : self-inductance of short circuit coil.
L_{sa1} and L_{a1s} : mutual inductance between faulty coil$_{A1}$and shorted coil.

The inductances in above equations are differential inductance which is calculated by the derivative of the *ac* component of flux linkage versus the *ac* component of current in coil$_{A1}$. They are assumed to be calculated at the same saturation level and the amplitude of the *ac* sinusoidal current is limited. Thus the magnetic reluctance in the magnetic equivalent circuit can be considered as constant.

The resistance and self-inductance of the coil in faulty case decreases because of the change in turns. Furthermore, according to Faraday's law of induction, the current resulting from the electromagnetic induction generates opposite flux against the main flux. Therefore, the reactance components in

equation (2) decreases due to the electromotive force introduced by the circulating pass. If the excited coil in equation (2) is not the faulty coil but the coil linked with the circulating pass by flux lines, the opposite electromotive force also reduces the reactance of this coil.

In the multiple slots machine, there are multiple coils in one phase winding. Thus, the self-inductance of one phase consists of the self-inductance of each coils and the mutual inductance between coils in this phase. If all the coils have the same number of turns, the mutual inductance in healthy condition can be given by,

$$L_{Mutual} = k\frac{N_H^2}{R_m} \quad (4)$$

where L_{Mutual} is the mutual inductance of two coils; N_H is the number of turns for one coil in healthy condition; R_m is the magnetic reluctance; *k is* the coefficients corresponds to the flux distribution between coils. In three phase machines, the directions of the flux generated by coils in one phase are close to each other. Therefore, if inter turn short circuit fault happens, the absolute value of mutual inductance reduces. Hence, it decreases the reactive component induced by the coupling of in-phase coils.

The mutual inductance of coils in different phases can also be written as in equation (4). In the three phase machines, the flux generated by different phase windings is shifted by 120 electrical degrees. Therefore, different phase windings generates opposite flux components in other phases when they are excited identically. In the case of inter turn short circuit fault, the faulty coil generates less flux due to the decrease in effective number of turns. However, because the current can be different in the three phase windings, the voltage induced by coupled coils of different phases change depending on the current. The current phase shift at steady state is hard to calculate precisely due to the multiple coupled inductors. Therefore, two special situations are analyzed here: i) the current in faulty and healthy coils have identical phase shifts. In this case, when a fault exists, the absolute value of mutual inductance decreases. Therefore, the voltage induced by the coupling coils decreases. ii) the current in faulty and healthy coil have 180 degree phase shift. Under this condition, the induced voltage increases and the reactive component at the terminals decrease.

B. Analysis of d-axis Impedance

A typical two level inverter topology is used during the implementation. Initially, it is designed to analyze the winding impedances through injected signals using a 2.5kW motor drive. For this purpose, the rotor is locked to a 0, 120 or 240 degree electrical angle by applying positive *dc d*-axis current for these positions. Next, the coils are excited by a combination of *dc* and relatively small *ac* signals where *dc* (*d*-axis current) is responsible from position stabilization and saturation level adjustment and the *ac* signal is used to measure the winding impedances. According to *dq0* transformation, if the constant factor is neglected, the equivalent electrical circuit of *d*-axis at different positions can

be derived easily; the *d*-axis equivalent circuit of 0 degree is equal to phase A series with the parallel circuit of phase B and C; the *d*-axis equivalent circuit of 120 degrees is equal to phase B series with the parallel circuit of phase A and C; the *d*-axis equivalent circuit of 240 degree is equal to phase C in series with the parallel circuit of phase A and B. The reason why the motor are tested at different position is the mutual inductance variation in faulty condition. As the analysis in last section, the voltage induced by coupling coils in different phases depends on the current phase shift. Consider the inter turn short circuit fault happens in phase A winding. If *ac* current is injected from phase A to phase B and phase C (the *d*-axis is at 0 degree), the phase A current will have 180 degree phase shift to other phases current. According to previous analysis, the voltage induced by coupling coils decreases in this case. Since both the resistance and self-inductance reduce, the equivalent impedance seeing from the terminals decreases. If *ac* current is injected from phase B winding, phase A winding and phase C winding are parallel. (the *d*-axis is at 120 degree) Hence the phase A current has little phase shift to phase C current and the voltage induced by coupling coils between the two phases increase. Thus, in this case, the stator winding impedance drops less comparing to the previous situation.

Here, *ac* signal amplitude is selected as fraction of rated current on purpose to make sure that it doesn't affect the core saturation. In addition, the frequency of the *ac* signal is set to rated frequency of the motor to make sure that the analyses are done within operation bandwidth and based on the actual impedance values. In order to measure the stator winding impedance, *dc* and sinusoidal *ac* signals are generated by the motor drive. Only the sinusoidal current and voltage are used to calculate the impedance and the *dc* signal can be eliminated by averaging. If the electrical angle of the applied field is *0* degrees, the equivalent impedance of the stator winding can be calculated by the line to line voltage and the phase A current.

$$Z_{total(0)} = \frac{\vec{V}_{l-l(0)}}{\vec{I}_{a(0)}} \tag{5}$$

Through above equation, the impedance seen at terminal or the *d*-axis impedance can easily be calculated by rms value of line to line voltage and phase current. Initial condition value of healthy motor impedance at different excitation level is required. It is used as the reference of the fault classification. Due the imperfection of manufacture, the stator windings of healthy machines also have inherent unbalance. Therefore, the definition of impedance variance threshold to make fault decision is different for different machines.

III. DIAGNOSIS OF INTER TURN SHORT CIRCUIT FAULT IN PMSMs

As the above analysis shown, the impedance of the motor stator winding can be estimated by the *d*-axis voltage and current. However, in PMSMs, the influence of saturation caused permanent magnet should be considered. Based on the analysis of saturation, the method to classify the inter turn
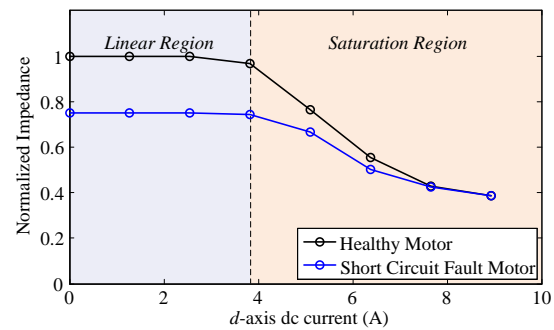

Fig.4. Simulation result of inter turn short circuit fault motor.

short circuit and eccentricity faults is discussed in this section. Corresponding 2-D FEA simulations are performed in ANSYS Maxwell environment to verify the analysis.

A. Saturation Effects Caused by PMs in Diagnosis and Classification

In PMSM motors, the influence of permanent magnet should be considered in detail for stator winding impedance calculations. The magnetic field generated by permanent magnet makes the magnetic operating point of iron core close to the knee region of the BH curve. As a result, the differential inductance of *d*-axis will drop if further excitation field is applied aligned with the permanent magnet field. This additional field can be established by injecting a positive *dc* current in *d*-axis.

In PMSM, the relationship between magnetic inductance and magnetic reluctance of iron core and air gap can be approximated as the following equation,

$$L_m = \frac{N^2}{R_m} = \frac{N^2}{\dfrac{l_c}{\mu_r \mu_0 A_c} + \dfrac{l_g}{\mu_0 A_g} + R_{pm}} \tag{6}$$

where l_c, l_g, A_c and A_g are average iron core length, air gap length, average iron core area and air gap area respectively, μ_r and μ_0 are the relative permeability of the iron core and the permeability of vacuum and R_{pm} is the magnetic reluctance of the permanent magnets. Typically, μ_r has a large value and hence the first term in the denominator of (6) can be neglected when the iron core is not saturated. As the iron core saturated, μ_r decreases drastically and then converges to a constant value in the deep saturation region. In inter turn short circuit fault case; the mechanical structure of the PMSM remains the same as in the healthy case. In the linear region, the differential inductance has relatively constant value. If the magnetic field increases up to deep saturation region, the differential inductance decreases and then converges to a stable value again. In inter turn short circuit fault case; the mechanical structure of the PMSM doesn't change and hence, in the linear region, the differential inductance remains stable. If the magnetic field goes up to the deep saturation region, the differential inductance converges to a relatively stable value again. Disregarding the temperature effect, the impedance with increasing magnetic field in both healthy and short circuit fault 2-D FEA simulation results are given in Fig.4. In this simulation, 21 turns are shorted out of 71 of coil$_{A1}$.
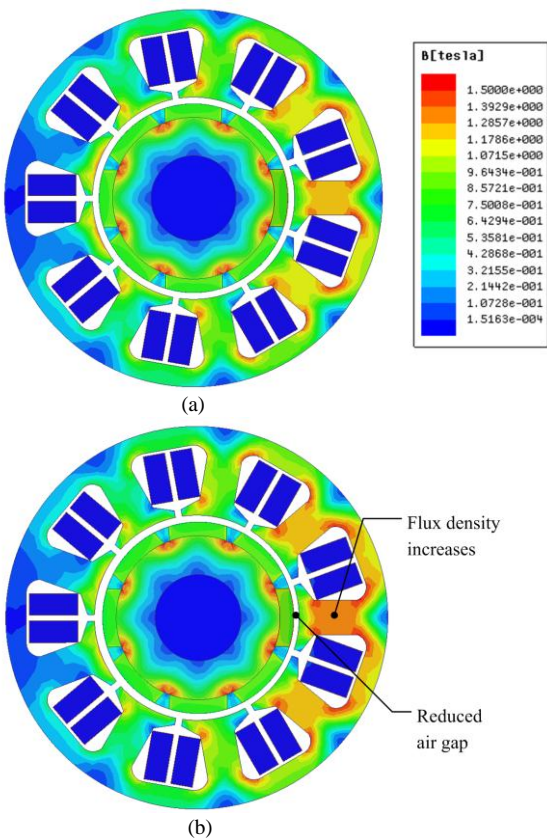
(a)

(b)

Fig.5. Saturation effect caused by eccentricity fault, (a) Healthy motor; (b) 20% eccentricity.

B. Analysis of Short Circuit Fault and Static Eccentricity Fault

According to [38] and above analysis, the d-axis impedance decreases when magnetic field strength increases in both static eccentricity and inter turn short circuit fault. However, the impedance in both cases exhibit different behaviors.

In inter turn short circuit fault, the mechanical structure of motor does not change. Therefore, both the faulty and healthy cases are expected to operate around the same magnetic operating point of the iron core. According to (6), when the magnetic field is in linear region, the magnetic reluctance of iron core can be neglected. The difference between d-axis impedance in healthy and faulty cases remains the same since the difference between the number of turns is constant. When the magnetic field increases up to the knee point and saturation region, the magnetic reluctance also increases which leads to the decrease in inductance difference. The impedance difference between the healthy and short circuit fault motor reduces as the magnetic field goes up.

In static eccentricity fault, the change of motor magnetic equation (6), the differential inductance with narrow air affects the magnetic operating point of the iron core. The 2D FEA simulation of eccentricity fault configuration is shown in Fig.5. Here, the minimum air gap appears at the 0 degrees and the magnetic field strength increases since the permanent magnet is closer compared to the healthy case. Thus in narrow air gap area, the operating point of iron core moves toward the saturation region. On the contrary, it is close to the linear region in wide air gap area.
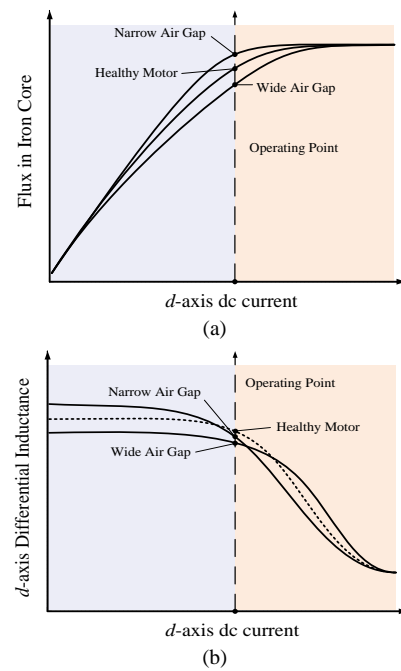

(a)

(b)

Fig.6. (a) Iron core flux versus d-axis dc current for eccentricity fault motor and healthy motor. (b) d-axis differential inductance versus d-axis dc current for eccentricity fault motor and healthy motor.
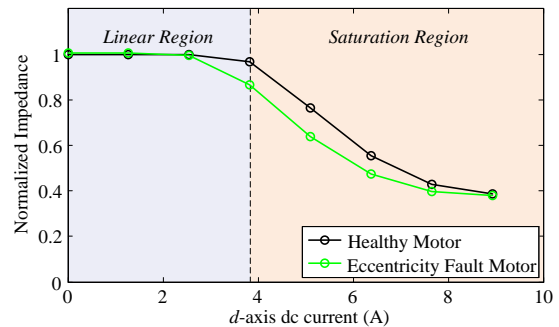

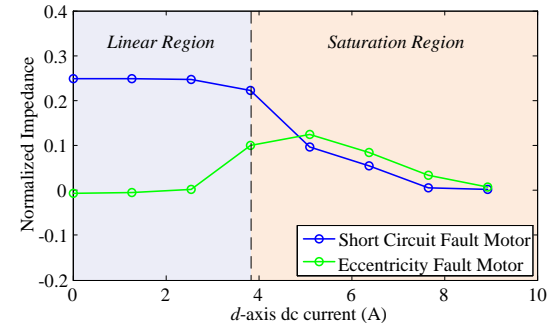Fig.7. Simulation result of eccentricity fault motor.

Fig.8. Impedance difference of inter turn short circuit motor and eccentricity fault motor.

If the magnetic field introduced by the permanent magnet in the narrow air gap area is not strong enough to drive the iron the core into saturation region, the flux, differential inductance and the d-axis dc current can be plotted as Fig.6. According to equation (6), the differential inductance with narrow air gap is greater than healthy one in linear region, but with the increased flux, the saturation leads to a decrease in differential inductance with zero dc current. Then, through increasing the d-axis current, it drops earlier than healthy case since the iron core starts to saturate rapidly.
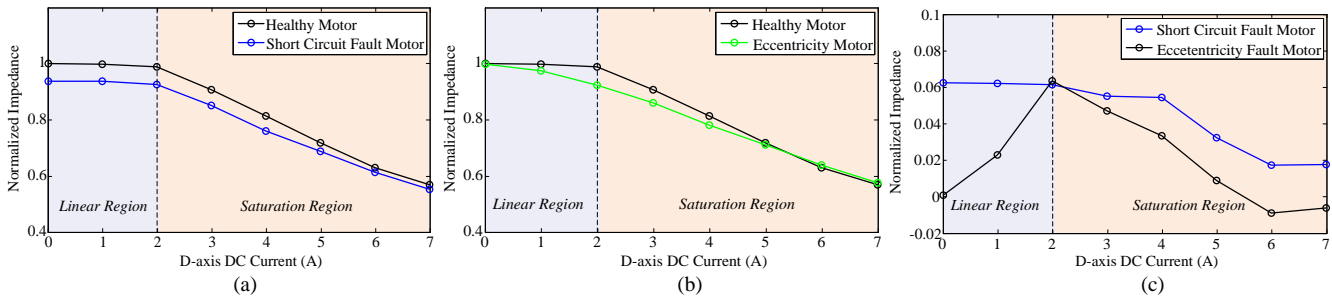
Fig.9. Simulation results of 4 poles/15 slots machine; (a) Healthy motor and short circuit fault motor; (b) Healthy motor and eccentricity fault motor; (c) Impedance difference of short circuit fault motor and eccentricity fault motor
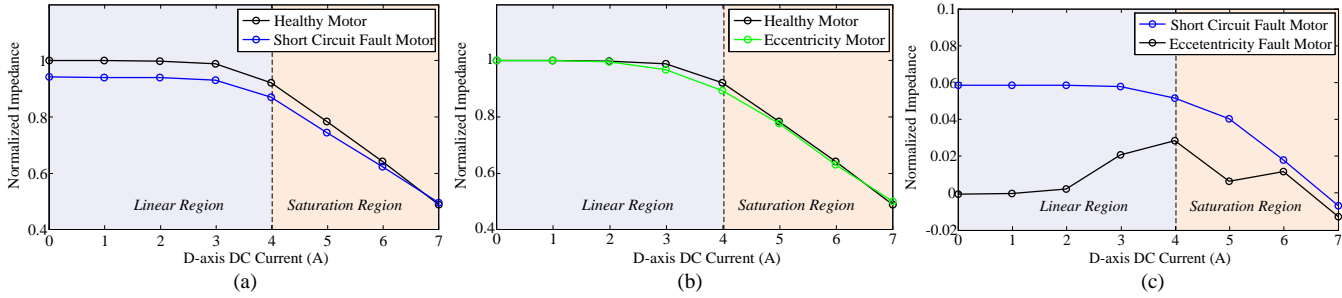

Fig.10. Simulation results of 6 poles/18 slots machine; (a) Healthy motor and short circuit fault motor; (b) Healthy motor and eccentricity fault motor; (c) Impedance difference of short circuit fault motor and eccentricity fault motor
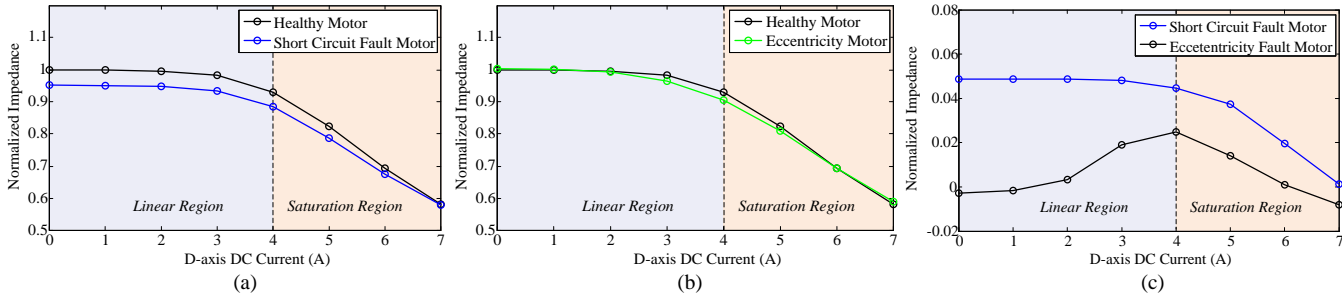

Fig.11. Simulation results of 8 poles/24 slots machine; (a) Healthy motor and short circuit fault motor; (b) Healthy motor and eccentricity fault motor; (c) Impedance difference of short circuit fault motor and eccentricity fault motor

TABLE I
DIFFERENT STATOR WINDING IN FEA SIMULATION

Pole/Slot	8/9	4/15	6/18	8/24
Coil Pitch	1	4	3	3
Symmetry	asymmetric winding	asymmetric winding	symmetric winding	symmetric winding
Winding Type	concentrated winding	distributed winding	distributed winding	distributed winding

Similarly, the differential inductance of wide air gap area decreases in linear region and drops later in saturation region. Furthermore, as large dc current is injected into d-axis, the curve of differential inductance in all cases merge together and the differential inductances converge to a certain stable value [38]. Since the eccentricity doesn't change the stator winding structure, the effects on stator winding resistance can be neglected. Thus, based on above analysis, the impedance change behavior of static eccentricity in 2-D FEA simulation can be described as in Fig.7.

In the simulation of eccentricity fault, the rotor is off-centered toward phase A by 20% of the air gap and the operating point of the iron core with zero excitation is set to the linear region. In Fig.7, it is clear that the d-axis impedance of eccentricity fault is almost the same as the healthy case with zero dc excitation current. As the d-axis current increase, it drops earlier compared to the healthy case between healthy and faulty cases. When the dc current leads to saturation in iron core, impedance difference raises to a larger value. the saturation level is further increased, the impedance difference drops.

When Fig.4 and Fig.7 are compared, it is possible to distinguish the inter turn short circuit fault and static eccentricity fault by observing the d-axis impedance change along through increase in the excitation current on d-axis. The impedance change can be calculated by subtracting that of faulty and healthy cases. In short circuit fault, the impedance variance between healthy and faulty motor remains the same with low excitation current, and then decreases when the iron core is deeply saturated.
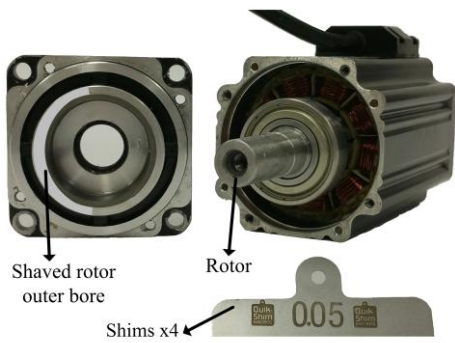
This article has been accepted for publication in a future issue of this journal, but has not been fully edited. Content may change prior to final publication. Citation information: DOI 10.1109/TIA.2016.2626264, IEEE Transactions on Industry Applications

7

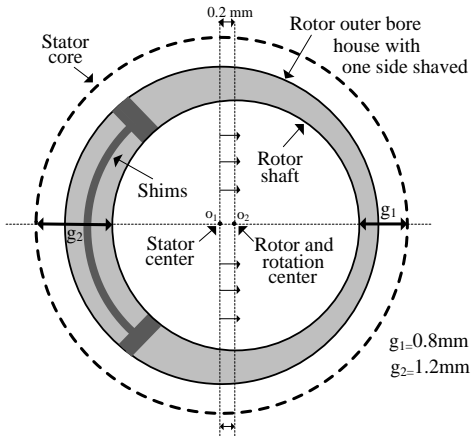Fig.12. Experimental setup of eccentricity motor. (20% eccentricity)

Fig.13. The shaft view of the mechanical design of eccentricity fault motor. (20% eccentricity)

On the contrary, it has tendency to increase before impedance difference drops for the healthy and eccentric motor. The simulation results shown in Fig.8 exhibits the same conclusion.

In order to verify the topology independence, different pole/slot combinations of PM synchronous machines are tested in FEA simulation. The designs of the stator windings covers different categories, including coil pitch, symmetry and winding distributions, as shown in Table I. The simulation results are given from Fig.9 to Fig.11.

IV. EXPERIMENT RESULTS

A. Experimental Setup

The experimental studies are implemented on a 2.5 kW, 8 pole surface mounted PMSMs and motor drive using the TMS320F28335 MCU. Several test motors are modified in through special machining to obtain inter turn shorts and eccentricity fault conditions. In the experiment, the *dc* current is adjusted from 0 A to 4.6 A. The peak value of *ac* sinusoid current is 0.5 A and the frequency is 200 Hz which is also the rated frequency of the motor. In order to avoid the damage caused by the heat in circulated coils, the excitation is applied for 30 seconds in each measurement to provide enough cooling time. The execution time of the proposed method takes no more than 470 instruction cycles, which is 3% of the total clock cycles of one sampling period when a 150MHz microcontroller is used at a 10 kHz switching frequency.
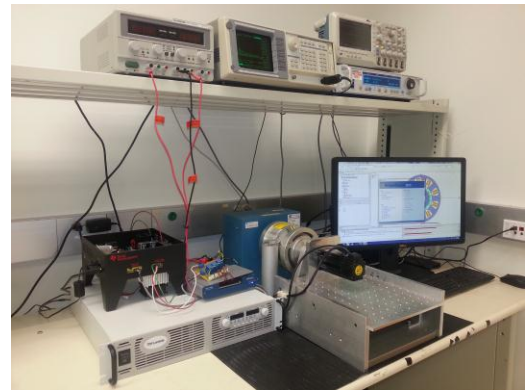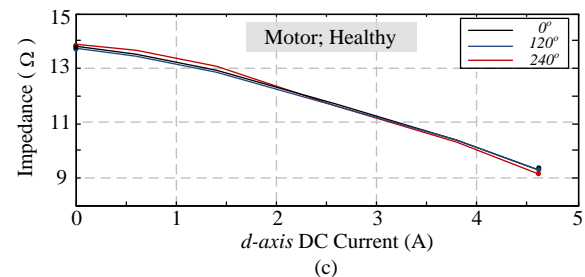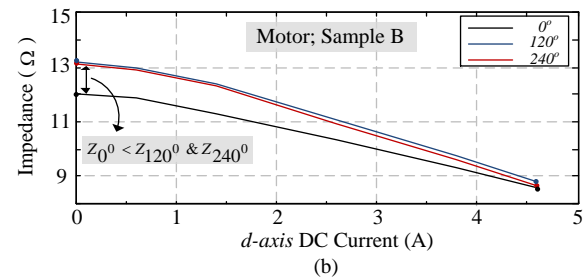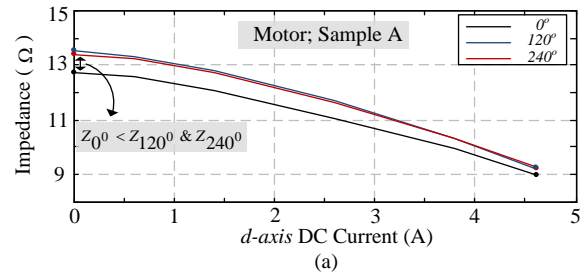

Fig.14. Experimental setup

Fig.15. *d*-axis impedance of inter turn short circuit fault at different positions, (a) Sample A; (b) Sample B; (c) Healthy motor.

The motor has 71 turns in one coil and 213 turns in one phase windings. In order to implement inter turn short circuit fault, the phase A windings are shorted by 8 and 21 turns in motor samples A and B. The faulty severity of inter turn short circuit fault are 3.75% and 9.85%. For eccentricity fault, motor hull is modified as in Fig.12 and Fig.13. The average air gap of a healthy motor is 1*mm*. In eccentricity fault, the upper side ring of the hull is shaved smoothly with maximum length of 0.2 *mm* for 20% eccentricity fault and 0.4 *mm* for 40% and iron shims are processed and filled in the lower ring for compensation. For motor samples C and D, they are modified with 20% eccentricity where the minimum gap appears at 120 degree of electrical angle and 40% eccentricity appears at 240 degree. The system setup is shown in Fig.1.
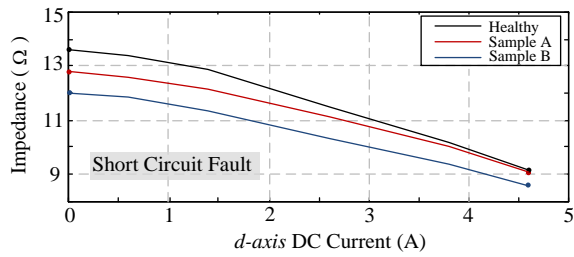
Fig.16. *d*-axis impedance of sample A, sample B and healthy motor on 0 degree.

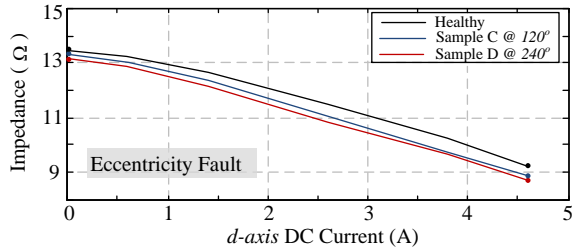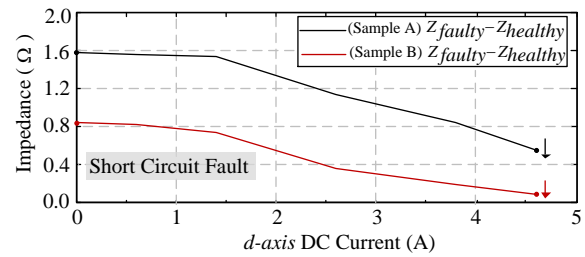

Fig.17. d-axis impedance of eccentricity fault motor and healthy motor at minimum air gap position. Sample C and healthy motor on 240 degree; Sample D and healthy motor on 120 degree.

Fig.18. *d*-axis impedance variance of inter turn short circuit motor and eccentricity fault motor at minimum air gap position, (a) Impedance of healthy motor subtract the impedance of inter turn short circuit fault; (b) Impedance of healthy motor subtract the impedance of eccentricity fault motor at minimum air gap position.

B. Experimental Results

The experimental results of motor A and B at different rotor positions are given in Fig.15. Both motors have the short circuit fault in phase A winding. In Fig.15, one can see that the *d*-axis impedance measured at *0* degrees is much less than the impedance measured at other two positions, especially at low saturation level. The reason is the phase A winding is in series with the paralleled two healthy windings. As the short circuit appears, both the self-inductance and mutual inductance reduce and hence, the *d*-axis impedance decreases. However, at other positions, the faulty phase A winding is paralleled with the healthy winding, the decrease of *d*-axis impedance is not as obvious as 0 degree position. Thus the fault location can be identified through the impedance variance.

Similarly, this test is able to be used to obtain the threshold of the impedance variance of the healthy PM motors. Due to the imperfect manufacture, there must be the inherent unbalance in the motor. Therefore, it is important to distinguish the fault cases and the imperfections. By testing the healthy motor, the minor variance of the impedance can be observed at different positions, as shown in Fig.15 (c). Thus the threshold of the impedance variance of faulty condition can be calculated by averaging the absolute value of the impedance difference between each two phases.

The experimental results at the faulty position of inter turn short circuit fault motors, eccentric motors and healthy motor are given in Fig.16 and Fig.17. In Fig.16, it is obvious that the impedance of motor A and B are lower than the impedance of healthy motor. As the shorted turns increasing from 8 turns (sample A) to 21 turns (sample B), the decrease in impedance becomes higher. Regarding the *dc* excitation current, the impedance of all cases is becoming smaller as the excitation current increases. This phenomenon reveals the effect of iron core saturation which was discussed in the previous section. Fig.17 shows the impedance change of eccentricity fault motors in terms of the *dc* excitation current. Similar to the
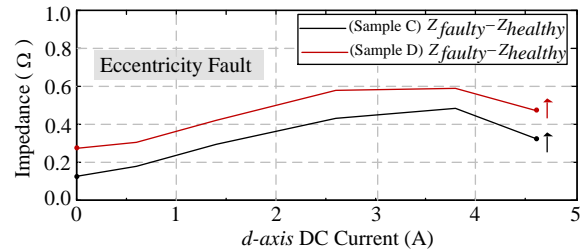
inter turn short circuit fault, the impedance of fault cases decreases as well.

However, per the analysis in the previous section, the impedance of the eccentric motor drops in a different manner compared to the short circuit fault. This can be better explained by the impedance difference between healthy and faulty cases as shown in Fig.18. In Fig.18 (a), the impedance difference between short circuit fault and healthy case is significantly higher when the excitation current is low. As the *d*-axis current increase, the iron core saturation level increases, the variance of the impedance decreases.

On the contrary, for the eccentricity fault, the impedance difference between faulty and healthy cases is relatively low when the excitation is low as shown in Fig.18 (b). The impedance variance increases through the saturation level. Finally, it decreases when the excitation current is large enough to saturate the iron in both cases. Thus, the impedance difference curve between eccentric motor and healthy motor has a peak value at a certain saturation level. The threshold of the impedance variance is also given in Fig.18. At low excitation level, the inter turn short circuit fault shows great difference of the impedance varience comparing the threshold. On the other hand, the eccentricity fault gives higher difference to the threshold at high saturation level.

V. Conclusion

In this paper, a PMSM inter turn short circuit fault diagnosis is explored through impedance estimation. In order to minimize false alarms, a discernment procedure is proposed for the inter turn short circuit and eccentricity faults which exhibit similar dynamic impedance behavior. The impedance difference of healthy and faulty motors is selected as the precursor to detect and classify these faults and the findings are verified through FEA simulations and experimental

analysis. Furthermore, the impedance change can be used to indicate the faulty phase winding and estimate the fault severity.

Compared to traditional methods, using the impedance difference has mainly two advantages. Firstly, it provides reliable way to distinguish the inter turn short circuit fault and eccentricity without considering the load/speed conditions. And this approach is not dependent to pole/slot combinations. Secondly, the impedance estimation method doesn't require additional or plug-in hardware, but relies on the readily available drive components. Furthermore, it can be implemented through algorithms which has very low computational burden. Thus, it is very practical and can be implemented on existing PMSMs drive systems easily as long as the user has access to micro-processing unit.

REFERENCES

[1] Gandhi, A.; Corrigan, T.; Parsa, L., "Recent Advances in Modeling and Online Detection of Stator Interturn Faults in Electrical Motors," in *Industrial Electronics, IEEE Transactions on* , vol.58, no.5, pp.1564-1575, May 2011doi: 10.1109/TIE.2010.2089937

[2] Cusido, J.; Romeral, L.; Ortega, J.A.; Rosero, J.A.; Garcia Espinosa, A., "Fault Detection in Induction Machines Using Power Spectral Density in Wavelet Decomposition," in *Industrial Electronics, IEEE Transactions on* , vol.55, no.2, pp.633-643, Feb. 2008

[3] J. K. Park and J. Hur, "Detection of Inter-Turn and Dynamic Eccentricity Faults Using Stator Current Frequency Pattern in IPM-Type BLDC Motors," in *IEEE Transactions on Industrial Electronics*, vol. 63, no. 3, pp. 1771-1780, March 2016.

[4] Seung-Tae Lee and Jin Hur, "Detection technique for stator inter-turn faults in BLDC motors based on third harmonic components of line currents,"*Energy Conversion Congress and Exposition (ECCE), 2015 IEEE*, Montreal, QC, 2015, pp. 1899-1904.

[5] Ebrahimi, B.M.; Faiz, J., "Feature Extraction for Short-Circuit Fault Detection in Permanent-Magnet Synchronous Motors Using Stator-Current Monitoring," in *Power Electronics, IEEE Transactions on*, vol.25, no.10, pp.2673-2682, Oct. 2010

[6] O. O. Ogidi, P. S. Barendse and M. A. Khan, "The detection of interturn short circuit faults in axial-flux permanent magnet machine with concentrated windings,"*Energy Conversion Congress and Exposition (ECCE), 2015 IEEE*, Montreal, QC, 2015, pp. 1810-1817.

[7] Barendse, P.S.; Pillay, P., "A New Algorithm for the Detection of Faults in Permanent Magnet Machines," *IECON 2006 - 32nd Annual Conference on IEEE Industrial Electronics,* Paris, 2006, pp. 823-828.

[8] Kyeong-Hwa Kim, "Simple Online Fault Detecting Scheme for Short-Circuited Turn in a PMSM Through Current Harmonic Monitoring," in *Industrial Electronics, IEEE Transactions on* , vol.58, no.6, pp.2565-2568, June 2011

[9] K. H. Kim, B. G. Gu and I. S. Jung, "Online fault-detecting scheme of an inverter-fed permanent magnet synchronous motor under stator winding shorted turn and inverter switch open," in *IET Electric Power Applications*, vol. 5, no. 6, pp. 529-539, July 2011.

[10] M. A. S. Nejad and M. Taghipour, "Inter-turn stator winding fault diagnosis and determination of fault percent in PMSM," *Applied Power Electronics Colloquium (IAPEC),* 2011 IEEE, Johor Bahru, 2011, pp. 128-131.

[11] J. Harsjo and M. Bongiorno, "Modeling and harmonic analysis of a permanent magnet synchronous machine with turn-to-turn fault," *Power Electronics and Applications (EPE'15 ECCE-Europe), 2015 17th European Conference on,* Geneva, 2015, pp. 1-10.

[12] T. Boileau, N. Leboeuf, B. Nahid-Mobarakeh and F. Meibody-Tabar, "Synchronous Demodulation of Control Voltages for Stator Interturn

Fault Detection in PMSM," in *IEEE Transactions on Power Electronics*, vol. 28, no. 12, pp. 5647-5654, Dec. 2013.

[13] S. T. Lee, K. T. Kim and J. Hur, "Diagnosis technique for stator winding inter-turn fault in BLDC motor using detection coil," Power Electronics and ECCE Asia (ICPE-ECCE Asia), 2015 9th International Conference on, Seoul, 2015, pp. 2925-2931.

[14] A. Sarikhani and O. A. Mohammed, "Inter-Turn Fault Detection in PM Synchronous Machines by Physics-Based Back Electromotive Force Estimation," in *IEEE Transactions on Industrial Electronics*, vol. 60, no. 8, pp. 3472-3484, Aug. 2013.

[15] B. Du, S. Wu, S. Han and S. Cui, "Interturn Fault Diagnosis Strategy for Interior Permanent-Magnet Synchronous Motor of Electric Vehicles Based on Digital Signal Processor," in *IEEE Transactions on Industrial Electronics*, vol. 63, no. 3, pp. 1694-1706, March 2016.

[16] B. G. Gu, J. H. Choi and I. S. Jung, "Development and Analysis of Interturn Short Fault Model of PMSMs With Series and Parallel Winding Connections," in *IEEE Transactions on Power Electronics*, vol. 29, no. 4, pp. 2016-2026, April 2014.

[17] J. Hang, J. Zhang, M. Cheng and J. Huang, "Online Interturn Fault Diagnosis of Permanent Magnet Synchronous Machine Using Zero-Sequence Components," in *IEEE Transactions on Power Electronics*, vol. 30, no. 12, pp. 6731-6741, Dec. 2015.

[18] Yongcan Li and Yongchun Liang, "A comparative study on inter-tern short circuit fault of PMSM using finite element analysis and experiment," *Advanced Mechatronic Systems (ICAMechS), 2015 International Conference on*, Beijing, 2015, pp. 290-294.

[19] Z. Qi and Y. Liang, "Evaluating the stator winding inter-tern short circuit fault of permanent magnet motor using FEA combined with experiment," *Electrical Machines and Systems (ICEMS), 2014 17th International Conference on*, Hangzhou, 2014, pp. 1034-1038.

[20] J. K. Park, C. L. Jeong, S. T. Lee and J. Hur, "Early Detection Technique for Stator Winding Inter-Turn Fault in BLDC Motor Using Input Impedance," in *IEEE Transactions on Industry Applications*, vol. 51, no. 1, pp. 240-247, Jan.-Feb. 2015.

[21] Gandhi, A.; Corrigan, T.; Parsa, L., "Recent Advances in Modeling and Online Detection of Stator Interturn Faults in Electrical Motors," in *Industrial Electronics, IEEE Transactions on* , vol.58, no.5, pp.1564-1575, May 2011

[22] J. A. Rosero, L. Romeral, J. Cusido, A. Garcia and J. A. Ortega, " On the short-circuiting Fault Detection in a PMSM by means of Stator Current Transformations," *Power Electronics Specialists Conference, 2007. PESC 2007. IEEE*, Orlando, FL, 2007, pp. 1936-1941.

[23] M. A. Awadallah, M. M. Morcos, S. Gopalakrishnan and T. W. Nehl, "Detection of stator short circuits in VSI-fed brushless DC motors using wavelet transform," in *IEEE Transactions on Energy Conversion*, vol. 21, no. 1, pp. 1-8, March 2006.

[24] N. H. Obeid, T. Boileau and B. Nahid-Mobarakeh, "Modeling and diagnostic of incipient inter-turn faults for a three phase permanent magnet synchronous motor using wavelet transform," *Industry Applications Society Annual Meeting*, 2015 IEEE, Addison, TX, 2015, pp. 1-8.

[25] J. A. Rosero, L. Romeral, J. A. Ortega and E. Rosero, "Short-Circuit Detection by Means of Empirical Mode Decomposition and Wigner–Ville Distribution for PMSM Running Under Dynamic Condition," in *IEEE Transactions on Industrial Electronics*, vol. 56, no. 11, pp. 4534-4547, Nov. 2009.

[26] C. Wang, X. Liu and Z. Chen, "Incipient Stator Insulation Fault Detection of Permanent Magnet Synchronous Wind Generators Based on Hilbert–Huang Transformation," in *IEEE Transactions on Magnetics*, vol. 50, no. 11, pp. 1-4, Nov. 2014.

[27] Z. A. Ping, Y. Juan and W. Ling, "Fault Detection of Stator Winding Interturn Short Circuit in PMSM Based on Wavelet Packet Analysis," *Measuring Technology and Mechatronics Automation (ICMTMA), 2013 Fifth International Conference on,* Hong Kong, 2013, pp. 566-569.

[28] O. A. Mohammed, Z. Liu, S. Liu and N. Y. Abed, "Internal Short Circuit Fault Diagnosis for PM Machines Using FE-Based Phase Variable Model and Wavelets Analysis," *in IEEE Transactions on Magnetics*, vol. 43, no. 4, pp. 1729-1732, April 2007.

[29] W. G. Zanardelli, E. G. Strangas and S. Aviyente, "Identification of Intermittent Electrical and Mechanical Faults in Permanent-Magnet AC Drives Based on Time–Frequency Analysis," in *IEEE Transactions on Industry Applications,* vol. 43, no. 4, pp. 971-980, July-aug. 2007.

[30] E. G. Strangas, S. Aviyente and S. S. H. Zaidi, "Time–Frequency Analysis for Efficient Fault Diagnosis and Failure Prognosis for Interior Permanent-Magnet AC Motors," in *IEEE Transactions on Industrial Electronics*, vol. 55, no. 12, pp. 4191-4199, Dec. 2008.

[31] M. Zafarani, T. Goktas and B. Akin, "A simplified mathematical approach to model and analyze magnet defects fault signatures in permanent magnet synchronous motors," *Industry Applications Society Annual Meeting*, 2015 IEEE, Addison, TX, 2015, pp. 1-6.

[32] J. Arellano-Padilla, M. Sumner and C. Gerada, "On-line detection of stator winding short-circuit faults in a PM machine using HF signal injection," *Electrical Machines, 2008. ICEM 2008. 18th International Conference on*, Vilamoura, 2008, pp. 1-8.

[33] S. C. Yang, "On-Line Turn Fault Detection of Interior Permanent Magnet Machines Using the Pulsating-Type Voltage Injection," in *IEEE Transactions on Industry Applications* , vol.PP, no.99, pp.1-1

[34] J. Arellano-Padilla, M. Sumner and C. Gerada, "Winding condition monitoring schemefor a permanent magnet machine using high-frequency injection," in *IET Electric Power Applications*, vol. 5, no. 1, pp. 89-99, January 2011.

[35] J. Arellano-Padilla, M. Sumner and C. Gerada, "Condition monitoring approach for permanent magnet synchronous motor drives based on the INFORM method," in *IET Electric Power Applications*, vol. 10, no. 1, pp. 54-62, 1 2016.

[36] N. Leboeuf, T. Boileau, B. Nahid-Mobarakeh, N. Takorabet, F. Meibody-Tabar and G. Clerc, "Estimating Permanent-Magnet Motor Parameters Under Inter-Turn Fault Conditions," in *IEEE Transactions on Magnetics,* vol. 48, no. 2, pp. 963-966, Feb. 2012.

[37] Jongman Hong; Sang Bin Lee; Kral, C.; Haumer, A., "Detection of Airgap Eccentricity for Permanent Magnet Synchronous Motors Based on the d-Axis Inductance," *in Power Electronics, IEEE Transactions* on , vol.27, no.5, pp.2605-2612, May 2012

[38] Jongman Hong; Sanguk Park; Doosoo Hyun; Tae-june Kang; Sang Bin Lee; Kral, C.; Haumer, A., "Detection and Classification of Rotor Demagnetization and Eccentricity Faults for PM Synchronous Motors," in *Industry Applications, IEEE Transactions* on , vol.48, no.3, pp.923-932, May-June 2012

[39] Haddad, R.Z.; Strangas, E.G., "Detection of static eccentricity and turn-to-turn short circuit faults in permanent magnet synchronous AC machines," in *Diagnostics for Electrical Machines, Power Electronics and Drives (SDEMPED),* 2015 IEEE 10th International Symposium on Guarad, 2015, pp. 277-283.